INHERENT DAMPING DURING NONLINEAR SEISMIC RESPONSE

Dionisio Bernal

Civil and Environmental Engineering Department, Center for Digital Signal Processing, Northeastern University, Boston MA 02115

Abstract

Viscous damping has long served as a surrogate for the aggregate of non-damage dissipative mechanisms. When the seismic response is strongly nonlinear most of the energy is dissipated by hysteresis but a question that has lingered is whether the viscous model holds unchanged during plasticity. It is shown in this paper that data supported information on this question can be obtained by inspecting the rate of change of the base shear over time intervals of strong plasticity. The results suggest that the constants that specify the pseudo viscous model decrease when hysteretic dissipation is active.

Introduction

A question that arises when the response of buildings to strong earthquakes is evaluated is whether the model that is used to capture energy dissipation not associated with damage should remain unchanged or be modified when hysteretic behavior is activated (Chopra and McKenna 2016, Luco and Lanzi 2017, Lanzi and Luco 2018). This paper attempts to answer this question by interrogating data with a scheme that combines constraints from dynamic equilibrium with acceleration measurements. The scheme, which we will refer to as the Inherent Damping Nonlinear Behavior (IDNB) extractor is built on the idea that during strong nonlinear response there may be time intervals in which the derivative of the restoring base shear is small enough for the inherent damping (InD) behavior to be ascertained by inspecting the derivative of the inertial base shear. As one gathers from the foregoing statement, a requirement for IDNB to operate is that one be able to identify time intervals over which significant plastic action is taking place and for which the base shear from the restoring mechanism (which cannot be measured) has a small derivative. Strong nonlinear behavior does not guarantee the existence of these intervals, and it follows from this that IDNB can interrogate some, but not all the nonlinear response data sets. It is not difficult to see that a small derivative of the base shear is much more likely to be realized in the nonlinear response of buildings with a lateral load resisting system formed by moment frames than in those where the bulk of the lateral forces are taken by shear walls and for this reason the results later presented are for moment frame buildings. We note that that although the exclusion of data sets for shear wall buildings reduces the number nonlinear responses available for examination, this does not hinder the ability of IDNB to address the central question, namely, whether the empirical data points to coupling or no coupling between pseudo-viscosity and hysteresis.

This paper begins by outlining the theoretical basis of IDBN and continues by discussing issues that arise in the estimation of signals that are needed in the interrogation, but which are not measured directly. The criteria used to decide on intervals of strong plasticity where the base shear derivative may be adequately small is presented next. The approach developed, together with the scheme used to establish the linear damping model are tested in simulations in the next section and are shown to be adequately robust. Having established the merit of IDNB in simulations the paper moves to the section for which all prior work was carried out, namely, to the application of IDNB to strong motion response data sets from real buildings. A section commenting on the results obtained closes the paper.

Inherent Damping Nonlinear Behavior (IDNB) Extractor

Under the typical assumptions of finite dimensionality and viscous dissipation, equilibrium for base excitation requires that

$$M \ddot{y}(t) + C(t)\dot{u}(t) + R(t) = 0 \tag{1}$$

where $\ddot{y}(t) \in \Re^{q \times 1} = \text{vector of absolute accelerations}$, $\dot{u}(t) \in \Re^{q \times 1} = \text{vector of velocities relative to the ground}$, $M \in \Re^{q \times q} = \text{symmetric mass matrix}$, $C(t) \in \Re^{q \times q} = \text{symmetric damping matrix}$, which we allow to depend on time, and R(t) is the vector of restoring forces, with q = number of degrees-of-freedom in the model that replaces the building for analysis. In our particular case, where 2D response is assumed and the inertial coordinates are the horizontal translations of the levels, q is the number of floors. For convenience in the analysis that follows we pre-multiply by the inverse of the mass and write Eq.1 as

$$\ddot{y}(t) + M^{-1}C(t)\dot{u}(t) + M^{-1}R(t) = 0$$
(2)

We now replace Eq.2 with a scalar equation obtained by pre-multiplying by a vector of weights, $r^T \in \mathfrak{R}^{1 \times q}$, namely

$$r^{T}\ddot{y}(t) + r^{T}M^{-1}C(t)\dot{u}(t) + r^{T}M^{-1}R(t) = 0$$
(3)

Selecting r so the terms in Eq.3 are (mass normalized) shears in a given story, differentiating with respect to time, and introducing obvious notation writes

$$\dot{V}_{I}(t) + \dot{V}_{D}(t) + \dot{V}_{R}(t) = 0 \tag{4}$$

The most appropriate story level for capturing inelastic behavior is typically level 1, in which case r is the usual vector of ones and one can readily see that the derivative of the damping term in Eq.4 writes

$$\dot{V}_{D}(t) = r^{T} M^{-1} \left(C(t) \ddot{u}(t) + \dot{C}(t) \dot{u}(t) \right)$$

$$\tag{5}$$

Inspection shows that the second term of Eq.5 is identically zero for invariant damping and since one expects this term to be small relative to the first, in general, we neglect it and write

$$\dot{V}_D(t) \cong r^T M^{-1} C(t) \ddot{u}(t) \tag{6}$$

Designating the damping matrix for linear behavior as C_0 one can also write

$$\dot{V}_D(t) = \rho(t)r^T M^{-1} C_0 \ddot{u}(t) \tag{7}$$

where $\rho(t)$ is a scalar that enforces equality between Eq.6 and Eq.7. Taking

$$V_{D0}(t) = r^{T} M^{-1} C_0 \dot{u}(t)$$
 (8)

Eq.7 writes

$$V_D(t) = \rho(t)V_{D0}(t) \tag{9}$$

which shows that $\rho(t)$ can be viewed as a scaling of the linear damping that, as far as the story shear contribution goes, is equivalent to the (unknown) variation of the coefficients in the damping matrix. Substituting Eq.9 into Eq.4 one gets

$$\dot{V}_{I}(t) + \dot{\rho}(t)V_{D0} + \rho(t)\dot{V}_{D0} + \dot{V}_{R}(t) = 0$$
(10)

On the premise that during any significant inelastic excursion the distribution of plastic hinges is not changing much it appears reasonable to take the modulation as constant. With this assumption and \tilde{t} as any time segment of significant inelasticity one can write

$$\dot{V}_{I}(\tilde{t}) + \overline{\rho} \, \dot{V}_{D0}(\tilde{t}) + \dot{V}_{R}(\tilde{t}) \cong 0 \tag{11}$$

where $\bar{\rho}$ is the average modulation during the excursion. Assume, temporarily, that \tilde{t} has been selected. If estimates of all the signals in Eq.11 were available, one could use the equation to solve for the mean modulation, but this appears impeded by the fact that \dot{V}_R is given by

$$\dot{V}_{R}(t) = \sum_{\ell=1}^{q} \frac{dV_{R}}{du_{\ell}} \dot{u}_{\ell}(t) \tag{12}$$

and the fact that the partial derivatives in Eq.12 cannot be estimated from available measurements. It is possible to move forward, however, by noting that \dot{V}_R may be sufficiently small (in relative terms) during \tilde{t} so that an estimation of the modulation obtained as

$$\overline{\rho} = \arg\min_{\rho} \left\| \chi(\rho, \tilde{t}) \right\| \tag{13}$$

where

$$\chi(\rho,\tilde{t}) = \|\dot{V}_{I}(\tilde{t}) + \rho \dot{V}_{D0}(\tilde{t})\|$$
(14)

may be reasonable. While one expects the average modulation in any given cycle to depend on the plastic hinge distribution, identification of modulations for specific yielding excursions is not a data-driven attainable goal so we settle for taking \tilde{t} as a vector containing all the time stations that one can, with reasonable confidence, assign to yielding excursions. The $\bar{\rho}$ obtained in this manner is then an average of sorts of the values that hold during the time stations in \tilde{t} . It's opportune to note that once a \tilde{t} vector is formed the answer to the minimization in Eq.13 follows readily as

$$\overline{\rho} = -\frac{\dot{V}_{D0}(\tilde{t})\dot{V}_{I}^{T}(\tilde{t})}{\dot{V}_{D0}(\tilde{t})\dot{V}_{D0}^{T}(\tilde{t})}$$

$$\tag{15}$$

We close this outline of IDNB by listing the expressions that, in Eq.11, are to be estimated from data, namely

$$\dot{V}_{I}(t) = r^{T} \ddot{y}(t) \tag{16}$$

$$\dot{V}_{D0}(t) = r^{T} M^{-1} C_0 \ddot{u}(t) \tag{17}$$

On the Selection of \tilde{t}

One gathers from the previous section that \tilde{t} is made up of time stations that belong to yielding excursions that have small \dot{V}_R values. Since \dot{V}_R cannot be estimated using Eq.12, we estimate it, instead, using Eq.11 for a set of $\bar{\rho}$ values that cover the feasible range and turn the problem into deciding which one of the estimates is "best". The idea is to extract time stations that are likely to be part of yielding excursions, for each trial modulation, and then select the modulation that maximizes the duration of \tilde{t} . To illustrate let the jth value of the possible modulations be $\rho_R(j)$. With this notation one has, from Eq.11

$$\dot{V}_{R}^{j}(t) = \dot{V}_{I} + \rho_{R}(j)\dot{V}_{D0}$$
(18)

designating

$$M_1^j = \max\left(\left|\dot{V}_R^j(t)\right|\right) \tag{19}$$

and

$$Z_1^j = all \, values \, of \, t \left| \frac{\left| \dot{V}_R^j \right|}{M_1^t} \le tol_1 \right| \tag{20}$$

with tol_1 being a small fraction (to be decided on) one gets a set of stations that have small values of \dot{V}_R . These stations, however, are not all contained in yielding excursions because the set includes also time stations that are in the vicinity of elastic unloading. Those that are connected to elastic unloading can be eliminated from the set by keeping only time stations for which the curvature of the restoring base shear is also small. To do so we take

$$M_2^j = \max\left(\left|\ddot{V}_R^j(t)\right|\right) \tag{21}$$

obtain

$$Z_2^j = \text{all values of } t \Big| \frac{\left| \ddot{V}_R^j \right|}{M_2^j} \le \text{tol}_2$$
 (22)

where tol_2 is also a small fraction and reduce the set to $Z_1^j \cap Z_2^j$. As a final requirement we compute

$$Z_3 = \text{all values of } t \left| \frac{|V_I|}{M_3} \ge tol_3 \right|$$
 (23)

where

$$M_3 = \max(\left|V_I(t)\right|) \tag{24}$$

where tol_3 is a substantial fraction and take the stations for the trial value of the modulation considered as

$$Z_4^j = (Z_1 \cap Z_2) \cap Z_3 \tag{25}$$

For the tolerances previously introduced we take, based on judgement and with some help from simulations, $tol_1, tol_2, tol_3 = 0.05, 0.3, 0.5$. Although it may that a time station that satisfies all the constraints has no neighbors (given the sampling rate) we decided to add the conservative requirement that only time stations that have neighbors remain in Z_4^j , e.g., if one has $Z_4^j = \{120,121,122,300,410,411,514\}$ the final set retained is $Z_5^j = \{120,121,122,410,411\}$. At the end of the process described one has one set of stations in Z_5 for each trial modulation. The final set, which defines \tilde{t} , is taken as the one that has the largest number of stations, and in case there is a tie between 2 or more, as the set that leads to the smallest value of the metric in Eq.14.

Reconstruction of Acceleration at Unmeasured Floors

Both Eqs.16 and 17 refer to accelerations at all levels of the building and since only some levels are measured the others have to be reconstructed. Much has been done in the area of response reconstruction and a suite of techniques that include some data-driven and some model-assisted ones of various levels of refinement are available (Kalman 1960; Hernandez and Bernal 2008; Bernal and Nasseri 2009a). Data-driven interpolators, which is the way we operate in this work, postulate a basis defined at all points of interest and (typically) solve for the generalized amplitudes by requiring that the product of the basis times these amplitudes match the measurements.

The reconstruction basis can be selected in different ways. One can, for example, expand eigenvectors identified at the sensors or expand some of the left side singular vectors of a data matrix (a matrix that lists measurements as its rows) or, quite conveniently, since no explicit expansion computations are involved, take the basis that a cubic spline interpolation implicitly selects. No matter how the basis is selected, however, the calculation of the generalized coordinates is key, and to discuss it we let q = # of levels in the building, $y \in \Re^{(q+1)\times 1}$ is the (albeit unknown except at sensor locations) response, including the ground, and $\Psi \in \Re^{(q+1)\times (q+1)}$ is an invertible matrix. With these definitions one can write

$$y = \Psi Y \tag{26}$$

or, in column partition form

$$y = \begin{bmatrix} \psi_1 & \psi_2 \end{bmatrix} \begin{Bmatrix} Y_1 \\ Y_2 \end{Bmatrix} \tag{27}$$

which is the same as

$$y = \psi_1 Y_1 + \psi_2 Y_2 \tag{28}$$

pre-multiplying Eq.28 by a diagonal row selector matrix $S \in \mathfrak{R}^{m \times m}$ that takes the measurements writes

$$y_m = S\psi_1 Y_1 + S\psi_2 Y_2 \tag{29}$$

where y_m are the measured coordinate. From Eq.29 one has

$$Y_{1} = (S\psi_{1})^{-1} (y_{m} - S\psi_{2}Y_{2})$$
(30)

To make Y_1 unique it is customary to take $\psi_1 \in \Re^{(q+1) \times m}$ so that $S\psi_1$ is square. Combining Eqs. 30 and 29 writes

$$y = \psi_1 (S\psi_1)^{-1} (y_m - S\psi_2 Y_2) + \psi_2 Y_2$$
(31)

The reconstruction that is consistent with the part of the measured response that projects on ψ_1 is thus

$$\tilde{y} = \psi_1 (S\psi_1)^{-1} (y_m - S\psi_2 Y_2)$$
(32)

which, of course, cannot be computed exactly because the second term in the parenthesis is not known. What is typically done in practice is to take the reconstruction as $\tilde{y} = \psi_1 (S\psi_1)^{-1} y_m$ which, as Eq.32 makes clear, projects response that belongs in ψ_2 unto ψ_1 . An improvement over this approach is to approximate the term in the parenthesis in Eq.32 by the measurements after they are filtered to the bandwidth covered by the 1-subspace. Referring to the low pass filtered version of the measurements as y_{mF} , namely

$$y_{mF} \cong (y_m - S\psi_2 Y_2) \tag{33}$$

the final reconstruction expression writes

$$\tilde{y} = \psi_1 \left(S \psi_1 \right)^{-1} y_{mF} \tag{34}$$

In the numerical work we take ψ_1 as the cubic spline basis for m measurements (Bernal and Nasseri 2009b).

Estimation of $M^{-1}C_0$

A very simple approach to estimate $M^{-1}C_0$ is to accept the approximation offered by mass proportional damping, in which case one has

$$M^{-1}C_0 = \alpha \cdot I \tag{35}$$

where α is given by

$$\alpha = 2\omega_{\ell}\xi_{\ell} \tag{36}$$

with ω and ξ being the radial frequency and the fraction of critical damping of the mode whose damping one decides to specify, typically the fundamental mode in the case of buildings.

A Data Consistent Approach

The approach described next is developed using accelerations velocities and displacements at all the coordinates and, as a consequence, carries approximation from the signal processing needed to obtain velocities and displacements from accelerations and from the fact that the accelerations at unmeasured floors are reconstructed. The last item limits the rank of the estimated damping to the number of measurements and although there are q - m undamped deformation patterns these have little effect on the performance of IDNB as they essentially span the higher modes. We begin by writing the dynamic equilibrium for base excitation on the premise of linear behavior, namely

$$\ddot{v} + M^{-1}C_0\dot{u} + M^{-1}Ku = 0 \tag{37}$$

and proceed by defining data matrices where each column is a time station, over p-time stations that need not be sequential, namely

$$\ddot{Y} = \begin{bmatrix} \ddot{y}_1 & \ddot{y}_2 & \dots & \ddot{y}_p \end{bmatrix} \quad \dot{U} = \begin{bmatrix} \dot{u}_1 & \dot{u}_2 & \dots & \dot{u}_p \end{bmatrix} \quad U = \begin{bmatrix} u_1 & u_2 & \dots & u_p \end{bmatrix}$$
(38)

and, using Eq.37 write

$$\ddot{Y} + M^{-1}C_0\dot{U} + M^{-1}KU = 0 (39)$$

Since the index p can be taken large compared to the number of floors the data matrices in Eq.38 can be made wide, and since all wide matrices have a right null space, it is always possible to find a matrix Z such that

$$UZ = 0 (40)$$

Post-multiplying Eq.39 by Z one gets

$$M^{-1}C_0\Upsilon = B \tag{41}$$

where

$$B = -\ddot{Y}Z \tag{42}$$

and

$$\Upsilon = \dot{U}Z \tag{43}$$

One can solve Eq.41 in a least square sense for $M^{-1}C_0$ but this option does not enforce the symmetry constrain that holds in most instances (since the mass matrix is usually proportional to the identity). One can enforce the constraint by operating with a solution format offered by the well-known property of the Kronecker product that allows one to write

$$(\Upsilon^T \otimes I) vec(M^{-1}C_0) = vec(B)$$
(44)

where \otimes =Kronecker product and $vec(\Box)$ is the vectorization operator, which creates a vector by stacking the columns of a matrix from left to right (Kaylath 1990). The symmetry of $M^{-1}C_0$ can be enforced by adding the columns corresponding to symmetric coefficients in the matrix of the *lhs* and solving for the unique coefficients or by adding the symmetry constraint equation and solving the larger system. We here opt for the second scheme and thus write the symmetry constraints as

$$S \cdot vec(M^{-1}C_0) = 0 \tag{45}$$

where $S \in \Re^{r_1 \times c_1}$ is a matrix where each row contains two non-zero values (1 and -1) and where $r_1 = 0.5q(q-1)$ and $r_2 = q^2$, combining Eq.44 and 45 one gets

Under the presence of noise and errors from reconstruction there is no guarantee that all the eigenvalues of the matrix in Eq.46 are positive. Small negative eigenvalues are of no consequence but can be eliminated, if deemed appropriate, by performing a spectral decomposition of $M^{-1}C_0$, replacing the negative eigenvalues with zeros and reassembling back.

InD Nonlinear Models

When IDNB is implemented errors come from a number of sources, namely: 1) the modulation is not necessarily constant during inelastic excursions, 2) there is error in the reconstruction of unmeasured levels, 3) there is error in the numerical differentiation of the absolute accelerations, 4) $M^{-1}C_0$ is computed using reconstructed data and is thus approximate, 5) estimation of the time stations that belong to \tilde{t} involves thresholds that require judgement and, most importantly, 6) the result is conditional on $\dot{V}_R(\tilde{t})$ being sufficiently small, which may or

may not be true for a given data set. Since the correct answers are not known when data from real buildings are considered, an appreciation of how IDNB performs can only be gained in simulations, and for this one has to decide on a nonlinear damping model. A brief review of some previously postulated models is presented next, and we conclude by describing the one that will be used in the numerical studies. The most widely used nonlinear model is a generalization of standard Rayleigh damping where C is taken as

$$C = \alpha M + \beta K_{T} \tag{47}$$

with α and β as constants and K_T = tangent stiffness matrix. Motivated by the perception that damping forces during significant nonlinear response appear too large, Hall introduced (Hall 2006) a model that has been designated as the capped model, the recommended limit on the damping force in this model is twice the damping ratio time the yield level. In 2017 Luco and Lanzi introduced a model where the damping matrix is taken as

$$C = C_0 K^{-1} K_T \tag{48}$$

where C_0 is any arbitrary damping matrix and K is the initial stiffness. Shortly after the appearance of the model in Eq.48 the same authors propose a modification that writes

$$C = K_T K^{-1} C_0 K^{-1} K_T (49)$$

which removes the lack of symmetry of Eq.48 and eliminates the possibility of negative eigenvalues. The last observation coming from the fact that the matrix in Eq.49 is a congruent transformation of C_0 and congruent transformations do not change the number of positive, negative and zero eigenvalues of a matrix. A feature common to all the previous models is that they cannot be modified in the plastic range without changing behavior when the response is linear. A model that has this ability is the CSMIP κ model, introduced in Bernal (2023) where the damping matrix is taken as

$$C = \left(\frac{\|K_T\|}{\|K\|}\right)^{\kappa} C_0 \tag{50}$$

where C_0 is arbitrary, κ is a free parameter and $\| \mathbf{l} \|$ stands for the 2-norm. As can be seen, when $\kappa = 0$ the model reverts to a constant damping matrix and as κ increases the magnitude of the reduction in the InD during the inelastic response increases.

The Nuclear Norm Ratio Model (NNRM)

The nuclear norm ratio model has the same form as Eq.42 with the only difference being that the 2-norm, which is the largest singular value, is replaced by the nuclear norm, which is the sum of all the singular values. Although we do not know from data that the nuclear norm is a better choice than the 2-norm, qualitative reasoning suggests that this may be so since this norm is less dependent on the spatial distribution of the plasticity. The expression in this case writes

$$C = \left(\frac{\left\|K_T\right\|_*}{\left\|K\right\|_*}\right)^{\kappa} C_0 \tag{51}$$

where $\parallel \parallel_*$ stands for the sum of the singular values. The simulations carried out in the numerical section use Eq.51 to model the inherent damping.

Numerical Validation

We begin by considering a SDOF system to illustrate how failure to satisfy the assumption that the base shear is flat during \tilde{t} affects the IDNB predictions. In this example we do not use Eq.51 but simply take $\rho = 1$ during linear response and $\rho = 0.5$ when the system is yielding, Furthermore, since there is no error from response reconstruction the tolerances used when selecting \tilde{t} can be set more tightly than for buildings and we thus take them as (0.01, 0.05 and 0.9). The SDOF chosen has a fundamental period of 1 sec and 5% damping when the response is linear. The restoring force vs relative displacement when the strain hardening slope is zero is depicted in Figure 1a and comparison between the IDNB identified modulation and the exact value is plotted in Figure 1b as the strain hardening increases. As can be seen, IDNB underpredicts $\bar{\rho}$ as hardening increases but the result is qualitatively acceptable throughout.

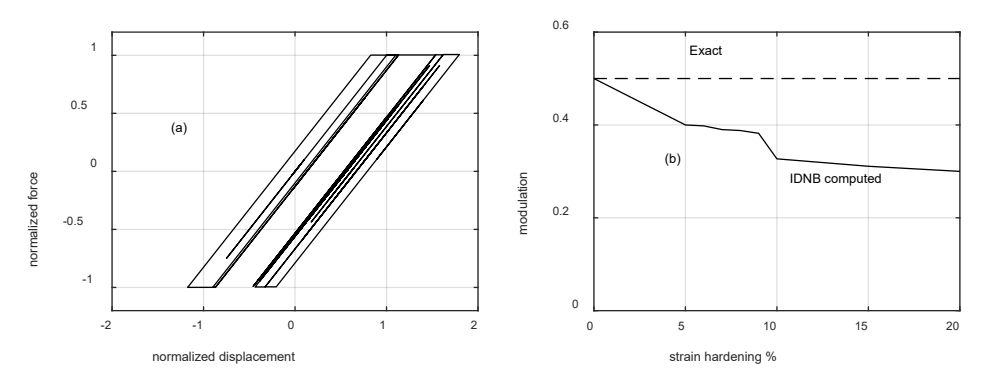


Figure 1. a) Force vs displacement during the response for the case of no strain hardening b) IDNB modulation prediction vs strain hardening (excitation is the record from channel 1 of CSMIP station 24386 during Northridge).

Results from IDNB on real buildings

Data from 6 buildings taken from the CSMIP database are used to determine the likelihood of coupling between pseudo-viscosity and hysteresis. As noted in the introduction, all the buildings have lateral forces resisting systems made up by moment frames. To accept a predicted modulation from IDNB we required that the result be stable with respect to 10% perturbations on the tolerances (around their selected nominal values of (0.05,0.3,0.5) and that the vector \tilde{t} contain stations from no less than two disjointed time intervals. These criteria were satisfied in 4 of the buildings selected but in station 57562, $\tilde{t} = \emptyset$ until tol_1 was increase to 0.1 and in 12299 there was only one nonlinear excursion until tol_1 was increased to 0.10. Table 1 lists the

CSMIP station #, the earthquake that generated the response treated as potentially nonlinear, the maximum recorded acceleration in the direction of analysis, the central 90% of the Arias intensity duration (Arias 1970), information on how the linear response used to compute the reference damping was obtained and the value of the modulation obtained when IDNB was used to interrogate the data. The plots from where the modulations noted are the minima are depicted in Figure 2.

		Channels psa ¹	InD for linear	Lateral Load	Modulation
Station	Earthquake	$t_{0.9}$	response	Resisting	$\overline{\rho}$
			computed using	System	
	Northridge	11,8,5,2 (0.865g)		Concrete	0.22
24322		8.54sec	Landers92	Frames	
		2,5,8 (0.579g)	last 32 secs of	Steel	0.69^{2}
57562	LomaPrieta	10.7sec	the motion in	Frames	
			column#2		
		1,3,12,11,10 (0.445g)	Last 24 secs of	Steel	0.17^{2}
12299	PalmSprings86	11.2 sec	the motion in	Frames	
			column#2		
		3,5,8,11 (0.448g)		Steel	0.49
24231	Northridge	11.8sec	Whittier87	Frames	
		13,12,11,10,9 (0.578g)		Concrete	0.66
24386	Northridge	12.1sec	BigBear92	Frames	
		14,13,12,11,10 (0.312g)		Concrete	0.61
24464	Northridge	13.54sec	Whittier87	Frames	

¹peak acceleration recorded on the channels used

² tol₁ relaxed to 0.1

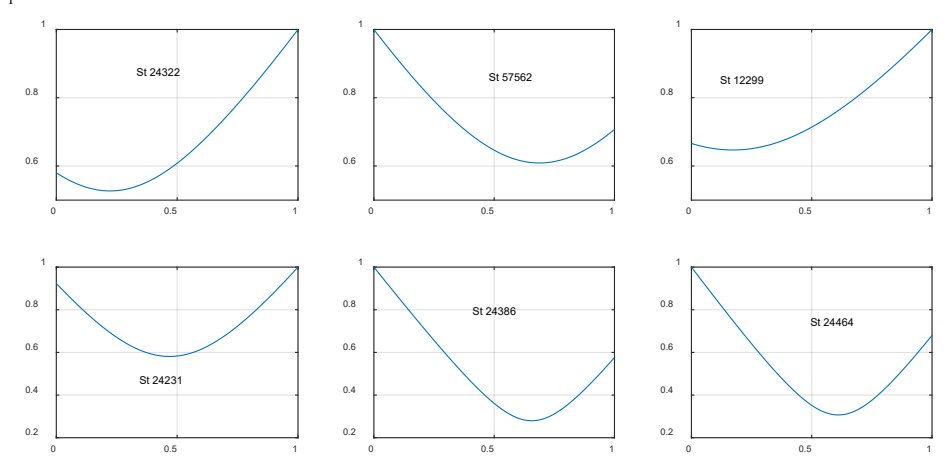


Figure 2. Normalized IDNB metric versus modulation for the cases in Table 1.

Concluding Observations

The results in Table 1 support the contention that the non-hysteretic related dissipation that takes place during plastic excursions is less than the value that an invariant pseudo-viscosity

model predicts. This result is consistent with the standard framework were damping ratios are assigned reasonable invariance within a structural type and material and the damping constants follow. Specifically, from this perspective one expects that the effectiveness of the pseudo-viscosity will decrease when the structure softens as a result of inelastic action, and this is what IDNB identifies. Accepting that there is a decrease in the pseudo-viscosity in the nonlinear case the question that opens up is how this should be handled in practice. While we have not done any systematic examination at the time or writing, our position (at this point) is that an approach that allows use of existing nonlinear codes without modification is likely justified. Specifically, it may be that it will be sufficient to state that if for linear analysis the viscous model is set up based on critical damping ratios equal to X% then for nonlinear time history analysis one should use some fraction (to be determined) of X.

Acknowledgement

The research reported in this paper was funded by the California Strong Motion Instrumentation Program (CSMIP) through standard agreement 1022-001. This support is gratefully acknowledged.

References

- Arias, A. (1970) "A measure of earthquake intensity in seismic design for nuclear power plants: R. J. Hansen, ed., MIT Press, pp.438-483.
- Bernal D., and A. Nasseri (2009a). "An approach for response reconstruction in seismic applications", Proceedings of the 3rd International Operational Modal Analysis Conference IOMAC09, Ancona Italy May 4-6.
- Bernal, D., and A. Nasseri (2009b) "Schemes for reconstructing the seismic response of instrumented buildings." SMIP09 Seminar on Utilization of Strong-Motion Data.
- Bernal, D., (2023) "Inherent Damping in Nonlinear Seismic Response", CSMIP Seminar.
- Caughey, T. K. (1960). "Classical normal modes in damped linear dynamic systems." *Journal of Applied Mechanics* 9
- Chopra, Anil K., and Frank McKenna (2016). "Modeling viscous damping in nonlinear response history analysis of buildings for earthquake excitation." *Earthquake Engineering & Structural Dynamics* 45 (2): 193-211.
- Hall, John F., (2006) "Problems encountered from the use (or misuse) of Rayleigh damping." *Earthquake engineering & structural dynamics* 35 (5): 525-545.
- Hernandez, E., and Bernal, D. (2008). "State estimation in systems with model uncertainties", *Journal of Engineering Mechanics*, ASCE, 252-257.
- Kalman, R. E. (1960), "A New Approach to Linear Filtering and Prediction Problems." *Journal of Fluid Engineering*, 82 (1): 35-45.
- Kaylath, T. Sayed A.H. and Hassibi b. (2000) Linear Estimation, Prentice Hall.
- Lanzi, Armando, and J. Enrique Luco (2018) "Elastic velocity damping model for inelastic structures." Journal of Structural Engineering 144 (6)
- Luco, J. Enrique, and Armando Lanzi (2017) "A new inherent damping model for inelastic time-history analyses." *Earthquake Engineering & Structural Dynamics* 46 (12): 1919-1939.